Appl. Phys. B 79, 883–889 (2004)
DOI: 10.1007/s00340-004-1642-z

Applied Physics B
Lasers and Optics

A. YOKOYAMA[1,✉]
H. OHBA[1]
M. HASHIMOTO[1]
K. KATSUMATA[1]
H. AKAGI[1]
T. ISHII[2]
A. OHYA[2]
S. ARAI[3]

Silicon isotope separation utilizing infrared multiphoton dissociation of Si_2F_6 irradiated with two-frequency CO_2 laser lights

[1] Department of Materials Science, Japan Atomic Energy Research Institute, 2-4 Shirakata, Tokai-mura, Naka-gun, Ibaraki 319-1195, Japan
[2] Nuclear Development Corporation, 622-12 Funaishikawa, Tokai-mura, Naka-gun, Ibaraki 319-1111, Japan
[3] Hill Research, 4-1-6 Roppongi, Minato-ku, Tokyo 106-0032, Japan

Received: 26 April 2004/Revised version: 6 August 2004
Published online: 29 September 2004 •

ABSTRACT Silicon isotope separation has been performed utilizing the infrared multiphoton dissociation (IRMPD) of Si_2F_6 irradiated with two-frequency CO_2 laser lights. The two-frequency excitation method improved the separation efficiency by keeping the high enrichment factors. For example, Si_2F_6 with the ^{28}Si fraction of 99.4% was obtained at 40.0% dissociation of Si_2F_6 after the simultaneous irradiation of 100 pulses with 966.23 cm^{-1} photons (0.089 J/cm^2) and 954.55 cm^{-1} photons (0.92 J/cm^2), while 1000 pulses were needed to obtain 99.0% of ^{28}Si at 27.2% dissociation in the case of single frequency irradiation at 954.55 cm^{-1} (0.92 J/cm^2). The single-step enrichment factors of ^{29}Si and ^{30}Si increased with increasing Si_2F_6 pressure. The reason for this enhancement has been discussed in terms of the rotational and vibrational relaxations by collisions with ambient gases.

PACS 42.62.Cf; 82.30.Lp; 82.50.Bc

1 Introduction

Natural silicon contains three stable isotopes: ^{28}Si, ^{29}Si, and ^{30}Si with the abundance ratio 0.9223 : 0.0467 : 0.0310. Recently, there has been much attention to use of enriched silicon isotopes in various fields [1]. For example, highly enriched ^{28}Si is interested in semiconductor field as a candidate for high thermal conductivity material to minimize the rise in temperature of the active areas of electronic and telecommunication devices [2], because silicon single crystal made of almost pure ^{28}Si, the atomic fraction of which is 99.85%, shows higher thermal conductivity than that made of natural silicon [2, 3].

Laser isotope separation is an attractive separation method, because a much higher enrichment factor can be achieved easily in comparison with other methods such as chemical exchange and gas-centrifugation. Silicon isotope separation has been studied utilizing isotopically selective IRMPD of SiF_4 [4] and Si_2F_6 [1, 5–10]. The isotope separation based on the IRMPD of Si_2F_6 is attractive, because Si_2F_6 can dissociate easily at lower laser fluence than SiF_4 and allows the irradiation of the molecules under nearly parallel laser beam condition. The parallel beam leads to large reaction zone in a cell and consequently a high dissociation rate. In addition, the isotopic selectivity obtained is much higher in Si_2F_6 than in SiF_4.

The high dissociation rate at low laser fluence is fundamentally important for practical large-scale isotope separation not only because of the increase in the isotope production rate but also because of the long-life operation of the laser. The improvement of the dissociation rate is expected by using multi-frequency irradiation method instead of the single frequency irradiation used in the previous studies, as has been reported in other isotopes [11–13]. The two-frequency irradiation consists of two successive excitation processes. At first, the desired isotopic molecules are selectively excited to quasi-continuum states by the irradiation at the nearly resonant frequency with a fundamental mode of the isotopic molecules and at very low fluence. Then, the isotopic molecules excited to the quasi-continuum states are dissociated by the irradiation at frequency suitable for the molecules in the quasi-continuum states but at relatively high fluence. This excitation scheme may improve not only the dissociation rate but also the isotopic selectivity, because the excitation of the undesired isotopic molecules resulting from the power broadening of the absorption lines at the first excitation stage is suppressed by the excitation at very low fluence. The silicon isotope separation using the two-frequency IRMPD of Si_2F_6 is examined in this work.

2 Experiment

Hexafluorodisilane was purchased from Mitsui Chemical Co. and used without further purifications. Only less than 2% of SiF_4 was detected as an impurity by an FT/IR spectrophotometer (JASCO FT/IR-410) and a GC/MS instrument (Shimadzu GCMS-QP2010). Because SiF_4 is easily produced by the reaction of Si_2F_6 with a trace amount of water that may present on walls of a gas cell and/or in a column of the GC/MS instrument, precise amount of SiF_4 in the purchased Si_2F_6 was not determined. Figure 1 shows the experimental arrangement used in this work. An irradiation cell (10 cm long and 2 cm i.d.) was made of stainless steel and equipped with NaCl end and side windows. Samples in the cell were irradiated at the repetition rate of 1 Hz by two CO_2 laser lights. A Lumonics TEA-841 CO_2 laser and an

✉ Fax: +81-29-282-5768, E-mail: atsushi@popsvr.tokai.jaeri.go.jp

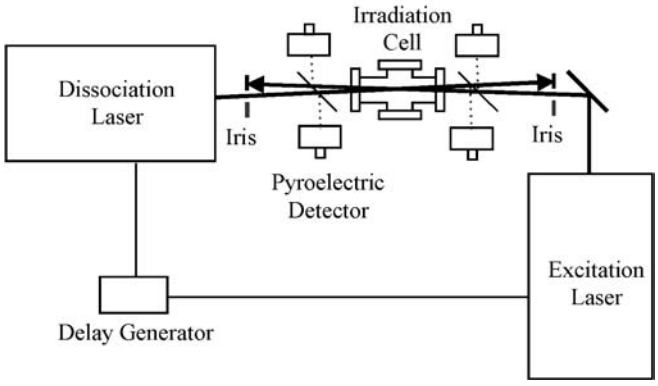

FIGURE 1 Experimental setup for the two-frequency irradiation experiment

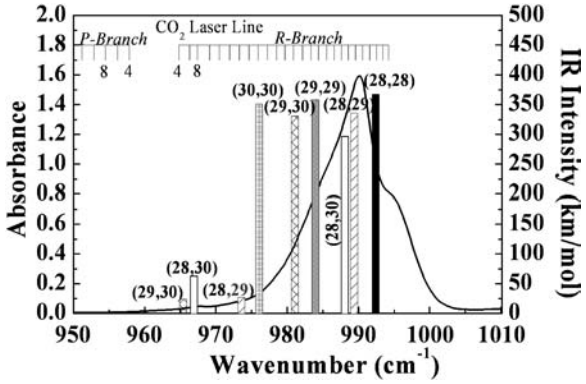

FIGURE 2 Fundamental frequencies and IR intensities for the ν_7 and ν_{10} modes of isotopic Si_2F_6. Numbers in parentheses indicate mass numbers of Si in Si_2F_6. The *solid curve* indicates the absorption spectrum for natural Si_2F_6

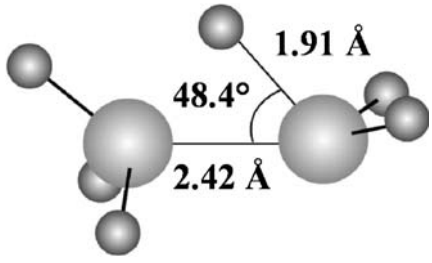

FIGURE 3 Transition state structure for reaction (1) calculated at B3LYP/6-31+G(d) level of theory

Ushio UGL-TEA-3C CO_2 laser were used as the excitation and dissociation sources, respectively. The laser beams were counter-propagating in the cell after having been collimated through an iris with a 1.5 cm diameter. The fraction of the overlap volume between two laser beams to the cell volume was estimated to be 0.35 ± 0.01. The pulse energy of each laser was monitored by splitting off a few percent of the beam to a pyroelectric joulemeter (Gentec ED-500). The pulse delay between two laser beams was set using a pulse delay generator (Stanford Research DG-535). The pulse shape of both laser beams is a spike of ca. 100 ns followed by a few μs tail. Concentrations of Si_2F_6 in the cell before and after irradiation were determined from absorbance of the absorption band around 990 cm^{-1}, which was measured through the side windows by using the FT/IR spectrophotometer. Although Si_2F_6 in the cell dissociated spontaneously to SiF_4 probably by the reaction with water in the cell, we conditioned the inside of cell so that Si_2F_6 in the cell dissociated at a rate of less than 0.3% per minute. Therefore, the spontaneous dissociation was neglected in the typical time for irradiation and analysis of the samples. Isotopic compositions of Si_2F_6 were determined from mass spectral peaks at $m/e = 151$ ($^{28,28}Si_2F_5^+$), 152 ($^{28,29}Si_2F_5^+$), and 153 ($^{28,30}Si_2F_5^+$) measured by a quadrupole mass spectrometer (ULVAC MSQ-400). Although $^{29,29}Si_2F_5^+$ is also observed at $m/e = 153$, the signal of the $^{29,29}Si_2F_5^+$ is much less than the $^{28,30}Si_2F_5^+$ in natural and irradiated Si_2F_6. Therefore, the contribution of the $^{29,29}Si_2F_5^+$ was neglected in the calculation of the isotopic compositions.

3 Results and discussion

3.1 *Isotope shift and dissociation mechanism of* Si_2F_6

Figure 2 shows an IR spectrum of Si_2F_6 from 950 to 1010 cm^{-1}. In this region, there exist two anti-symmetric SiF_3-stretching vibrations of Si_2F_6: ν_7 and ν_{10}. Naturally Si_2F_6 consists of $^{28,28}Si_2F_6$ (85.1%), $^{28,29}Si_2F_6$ (8.6%), $^{28,30}Si_2F_6$ (5.7%), $^{29,29}Si_2F_6$ (0.22%), $^{29,30}Si_2F_6$ (0.29%), and $^{30,30}Si_2F_6$ (0.10%). The frequencies of the anti-symmetric SiF_3-stretching modes for these isotopic molecules were calculated by an ab initio MO theory at B3LYP/6-31+G(d) level using a Gaussian 98 package [14] and tabulated in Table 1 along with the experimental values reported by Tosa et al. [15], the frequencies scaled with the scaling factors determined from the comparison with the experimental values, and the calculated IR intensities. When the isotopes of Si in Si_2F_6 are the same, the ν_{10} mode is inactive. If the isotopes of Si, however, are different, the ν_{10} mode becomes slightly active because of the breakdown of symmetry. Figure 2 also shows the calculated IR intensities of the ν_7 and ν_{10} bands and the CO_2 laser lines.

Unimolecular dissociation of Si_2F_6 produces SiF_4 and SiF_2 as follows:

$$Si_2F_6 \rightarrow SiF_4 + SiF_2 \,. \tag{1}$$

This reaction occurs through the three-center transition state shown in Fig. 3. The activation energy and the transition state were also calculated at B3LYP/6-31+G(d) level of theory. The calculated activation energy (187 kJ/mol) is consistent with the experimental value (193 ± 3 kJ/mol [16]). The SiF_2 products then polymerize to white solids. In this work, ^{29}Si and/or ^{30}Si are enriched in the products, and ^{28}Si is enriched in the residual Si_2F_6, because the Si_2F_6 containing ^{29}Si and/or ^{30}Si is selectively dissociated.

3.2 *Delay time dependence between excitation and dissociation laser pulses*

Figure 4 shows the plot of dissociation rate ${}^iW$ of the $^{28,i}Si_2F_6$ isotopic molecule as a function of time delay of the dissociation laser pulse, relative to the excitation laser pulse. The rate is defined as the fraction of $^{28,i}Si_2F_6$ dissociated per shot, and is related to the concentration of $^{28,i}Si_2F_6$, ${}^iN$, after the irradiation of n pulses as follows:

$${}^iN = {}^iN_0(1 - {}^iW)^n \,, \tag{2}$$

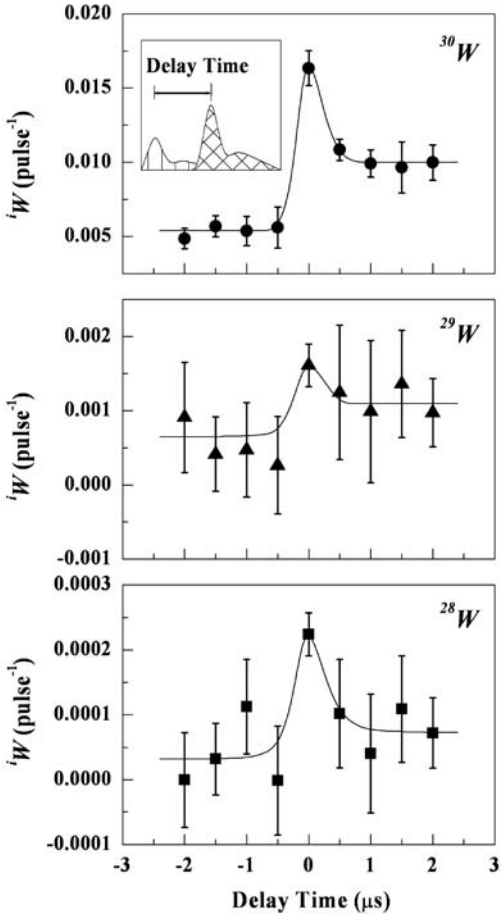

FIGURE 4 Pulse delay dependence of dissociation rates. The delay time represents the pulse delay of the dissociation laser pulse relative to the excitation laser pulse. Excitation and dissociation laser frequencies are 966.23 and 954.55 cm^{-1}, respectively. Excitation and dissociation laser fluences are 0.055 ± 0.001 and 0.953 ± 0.009 J/cm^2, respectively

where $^{i}N_0$ is the initial concentration of $^{28,i}Si_2F_6$. Since the overlap volume between two laser beams is smaller than the cell volume as described previously, the dissociation rate is smaller than the dissociation efficiency that is defined as the dissociation fraction of the molecules in the overlap region between the two laser beams. The dissociation efficiency per pulse is obtained by multiplying the dissociation rate by 2.86. The dissociation rate peaks at zero delay time and decreases to a constant value with increasing delay time. The dissociation rate is nearly constant at delay time from 1 to 2 μs. Although the excitation laser pulse has a 2 μs tail, the plateau of the tail ranges only from 0.2 to 0.3 μs. Therefore, the constant dissociation rate at delay time from 1 to 2 μs is not due to the overlap of the dissociation laser pulse with the tail of the excitation laser pulse but due to the deactivation of the excited molecules as a result of collisions with ambient molecules. This kind of delay time dependence is observed in the two-frequency measurements on average number of photons absorbed by OsO_4 [17] and CDF_3 [18]. A fraction of the molecules excited initially to the quasi-continuum states by the excitation laser can remain in the quasi-continuum states after the vibrational redistribution as a result of fast V–V exchange by collisions with cold Si_2F_6 molecules. Because the dissociation rate at negative delay is much smaller than

Mode	Si_2F_6	Calculated (cm^{-1})	Scaled (cm^{-1})	IR Intensity (km/mol)	Observed* (cm^{-1})
ν_7	$^{28,28}Si_2F_6$	961.2	992.3	367.1	992.3
	$^{28,29}Si_2F_6$	958.3	989.3	335.8	988.4
	$^{28,30}Si_2F_6$	957.1	988.0	296.2	
	$^{29,29}Si_2F_6$	953.1	983.9	358.5	
	$^{29,30}Si_2F_6$	950.3	981.0	330.9	
	$^{30,30}Si_2F_6$	945.5	976.0	350.4	
ν_{10}	$^{28,28}Si_2F_6$	948.4	979.0	0.0	979
	$^{28,29}Si_2F_6$	943.2	973.5	27.0	
	$^{28,30}Si_2F_6$	936.8	966.9	62.7	
	$^{29,29}Si_2F_6$	940.3	970.5	0.0	
	$^{29,30}Si_2F_6$	935.4	965.4	23.6	
	$^{30,30}Si_2F_6$	932.7	962.5	0.0	

*reference [15]

TABLE 1 Fundamental frequencies for the two anti-symmetric SiF_3 stretching modes of isotopic Si_2F_6 molecules

that at positive delay, the dissociation efficiency by the absorption of the dissociation laser photon is much larger for the molecules in quasi-continuum states than for the cold molecules. Because the maximum dissociation rate is obtained at zero delay time, other experiments under the two-frequency irradiation condition have been carried out at zero delay time.

3.3 *Laser frequency dependence*

The dependence of ^{i}W on the excitation laser frequency is shown in Fig. 5. The dissociation laser frequency was fixed to 954.55 cm^{-1}. The fluences of the excitation and dissociation lasers were 0.066 and 0.86 J/cm^2 at 2.0 Torr; and 0.054 and 0.91 J/cm^2 at 0.5 Torr, respectively. Although ^{28}W increases monotonically with increasing frequency, ^{29}W and ^{30}W have structures; ^{30}W shows a peak at 966.23 and ^{29}W has a shoulder at 973.29 cm^{-1}. Because these frequencies are consistent with ν_{10} mode frequencies of $^{28,30}Si_2F_6$ and $^{28,29}Si_2F_6$, respectively, the small enhancement of the dissociation rates at these frequencies is probably due to the ν_{10} mode excitation of $^{28,30}Si_2F_6$ and $^{28,29}Si_2F_6$. A single-step enrichment factor of silicon isotope i ($i = 29$ or 30), $^{i}\beta$ is defined as

$$ {}^{i}\beta = \frac{({}^{i}N_0 - {}^{i}N)/({}^{28}N_0 - {}^{28}N)}{{}^{i}N_0/{}^{28}N_0} = \frac{{}^{i}W}{{}^{28}W}. \qquad (3) $$

The enrichment factors $^{29}\beta$ and $^{30}\beta$ are also plotted against the excitation laser frequency in Fig. 6. The factors increase with decreasing laser frequency, because ^{28}W decreases faster than ^{29}W and ^{30}W, as a result of the larger difference between the fundamental and laser frequencies. The dependence of ^{i}W on the dissociation laser frequency is plotted in Fig. 7. The excitation laser frequency was fixed at 966.23 cm^{-1}. The fluences of the excitation and dissociation lasers were 0.062 and 0.74 J/cm^2, respectively. The dissociation rates increase with increasing frequency. This implies that the absorption peak of the molecules in the quasi-continuum states lies at higher frequency than 956.19 cm^{-1}. Unfortunately, we could not measure ^{i}W at higher frequency than 956.19 cm^{-1}, because of the lack of the CO_2 laser line.

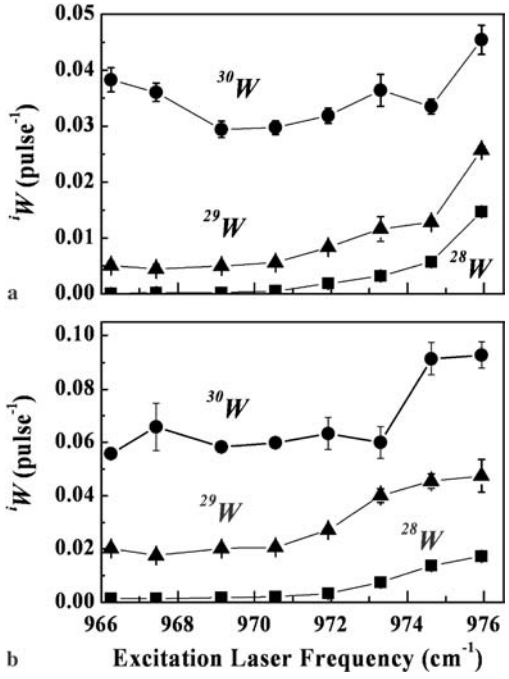

FIGURE 5 Dependence of dissociation rates ^{i}W on excitation laser frequency at the Si_2F_6 pressures of (**a**) 2.0 and (**b**) 0.5 Torr. Dissociation laser frequency is fixed at 954.55 cm^{-1}. Excitation and dissociation laser fluences are (**a**) 0.066 ± 0.003 and 0.86 ± 0.06 J/cm^2 and (**b**) 0.054 ± 0.003 and 0.91 ± 0.04 J/cm^2, respectively

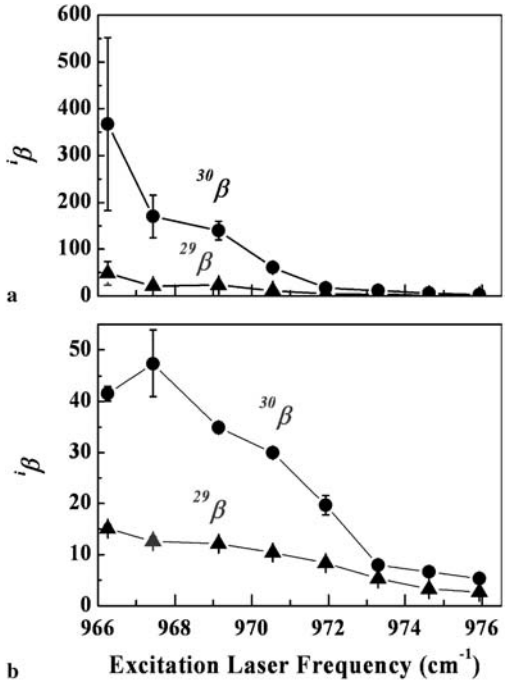

FIGURE 6 Dependence of enrichment factors $^{i}\beta$ in the dissociation products on excitation laser frequency at the Si_2F_6 pressures of (**a**) 2.0 and (**b**) 0.5 Torr. The laser frequencies and fluences are the same as those in Fig. 5

3.4 Ar *and* Si_2F_6 *gas pressure dependence*

The Ar pressure dependence of ^{i}W and $^{i}\beta$ is shown in Fig. 8. The Si_2F_6 pressure is kept at 0.5 Torr. The dissociation rate of $^{28,30}Si_2F_6$ is slightly enhanced, when the 0.5 Torr

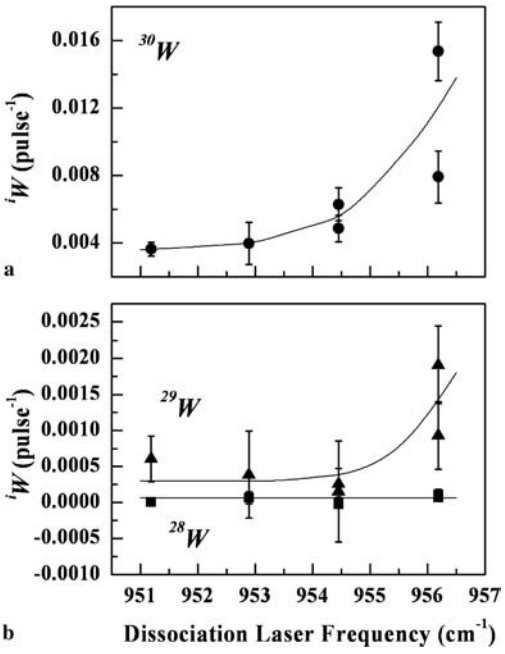

FIGURE 7 Dependence of dissociation rates ^{i}W on dissociation laser frequency at the Si_2F_6 pressures of 2.0 Torr. The excitation laser frequency is fixed at 966.23 cm^{-1}. The excitation and dissociation laser fluences are 0.062 ± 0.003 and 0.74 ± 0.08 J/cm^2, respectively

of Ar is added to Si_2F_6. This is due to the removal of the rotational bottleneck by the collisions of Si_2F_6 with Ar within the laser pulse. When the Ar pressure exceeds 0.5 Torr, the dissociation rate decreases with increasing Ar pressure as a result of the vibrational de-excitation induced by the collisions of the excited Si_2F_6 with Ar during the laser pulse. Because the Ar pressure dependence of ^{i}W is similar for $^{28,28}Si_2F_6$, $^{28,29}Si_2F_6$ and $^{28,30}Si_2F_6$, the enrichment factors change little with Ar pressure, as shown in Fig. 8. The Si_2F_6 pressure dependence of the dissociation rate is shown in Fig. 9. In this case no Ar was added. The dissociation rates decrease monotonically with increasing pressure as a result of the vibrational de-excitation induced by the collisions with Si_2F_6. However, the extent of the decrease is different between the isotopic Si_2F_6. The dissociation rate of $^{28,28}Si_2F_6$ decreases the most rapidly with increasing pressure. Therefore, the $^{30}\beta$ and $^{29}\beta$ values increase with increasing pressure as shown in Fig. 9. The enhancement of the enrichment factor by the increase in pressure has also been reported in the IRMPD of CF_3COCF_3 [19], CF_3Br [20, 21], and $CHClF_2$ [22]. In these cases, the enhancement of the enrichment factor was observed when the molecules were excited at the wings of the absorption peak as is the case of this study. Two explanations for the enhancement of the enrichment factor has been proposed: One is that the enhancement is due to the different behavior for the change in the rotational distributions for the desired and undesired isotopic molecules by collisions with buffer gas within the laser pulse duration; that is, the enrichment factor is enhanced when the dissociation rate for the desired isotopic molecules increases at larger extent than the undesired ones as a result of the removal of rotational bottleneck by the collision with buffer gases [21]. The other explanation is that the enhancement is due to the different behavior for the compe-

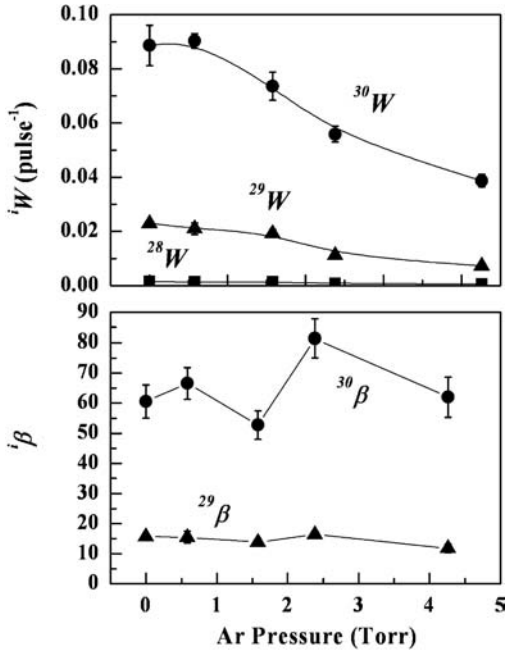

FIGURE 8 Dependence of dissociation rate ^{i}W and enrichment factor $^{i}\beta$ on Ar buffer gas pressure. The pressure of Si_2F_6 is kept at 0.5 Torr. The excitation and dissociation laser frequencies are 966.23 and 954.55 cm^{-1}, respectively. The excitation and dissociation laser fluences are 0.038 ± 0.002 and 1.04 ± 0.03 J/cm^2, respectively

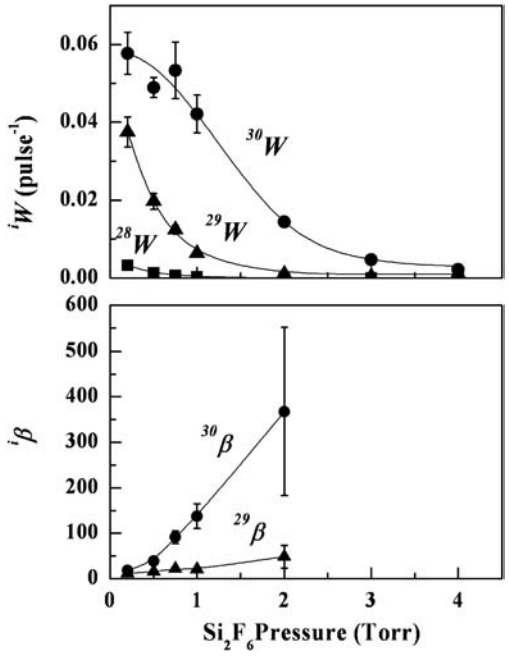

FIGURE 9 Dependence of dissociation rate ^{i}W and enrichment factor $^{i}\beta$ on Si_2F_6 pressure. No buffer gas is added. The excitation and dissociation laser frequencies are 966.23 and 954.55 cm^{-1}, respectively. The excitation and dissociation laser fluences are 0.046 ± 0.001 and 0.91 ± 0.01 J/cm^2, respectively

tition of the up-pumping with the vibrational de-excitation; that is, the decrease in the dissociation rate by vibrational de-excitation is smaller for the desired isotopic molecules than for the undesired ones, because the up-pumping rate of the desired isotopic molecules is much larger than that of the undesired isotopic molecules [20]. In the case of Si_2F_6, the removal of rotational bottleneck is minor contribution to the enhancement of the enrichment factors, because the addition of Ar buffer gas enhances only slightly the dissociation rate as shown in Fig. 8. Instead, the second explanation is plausible in the case of Si_2F_6. Since the excitation laser frequency is near the ν_{10} mode frequency of $^{28,30}Si_2F_6$ but 34 cm^{-1} apart from the absorption peak of $^{28,28}Si_2F_6$, the up-pumping rate and the vibrational temperature is expected to be much higher for $^{28,30}Si_2F_6$ than for $^{28,28}Si_2F_6$. This is supported by the average numbers of photons ($\bar{n}_{ph}$) absorbed by a molecule tabulated in Table 2 along with the state densities at the corresponding internal energy ($\bar{n}_{ph}h\nu_{ex}$), which were calculated from the fundamental frequencies tabulated in Table 1 by a direct counting method [23]. The $\bar{n}_{ph}$ values are estimated from the measured absorption coefficient at 0.068 J/cm^2 and $10R(6)$ line on the assumption that the absorption cross sections for the isotopic Si_2F_6 are proportional to the dissociation rates for the corresponding isotopic Si_2F_6. State density of $^{28,30}Si_2F_6$ at $\bar{n}_{ph}h\nu_{ex}$ indicates that a large number of the $^{28,30}Si_2F_6$ molecules are excited to the quasi-continuum states even at 0.067 J/cm^2. On the other hand, most of the $^{28,29}Si_2F_6$ and $^{28,28}Si_2F_6$ molecules remain in the discrete states. The average excitation level of the $^{28,28}SiF_6$ molecules especially is very low. Therefore, the effect of the vibrational de-excitation on the fraction of the molecules in the quasi-continuum states, which can absorb the dissociation laser photons, should be different between $^{28,30}Si_2F_6$ and $^{28,28}Si_2F_6$. In fact, the ratio of the dissociation yield at 1–2 μs delay to that at 0 μs delay is larger for $^{28,30}Si_2F_6$ (0.42 ± 0.04) and $^{28,29}Si_2F_6$ (0.53 ± 0.15) than for $^{28,28}Si_2F_6$ (0.22 ± 0.15) as shown in Fig. 4, which indicates that vibrational de-excitation from the quasi-continuum states to discrete states is less for $^{28,30}Si_2F_6$ and $^{28,29}Si_2F_6$ than for $^{28,28}Si_2F_6$.

3.5 *Laser power dependence*

Figure 10 shows the dependence of the dissociation rates and enrichment factors on the excitation laser fluence. The dissociation laser fluence is fixed at 0.90 ± 0.02 J/cm^2. The dissociation and excitation laser frequencies are 954.55 and 966.23 cm^{-1}, respectively. The dissociation rates for $^{28,30}Si_2F_6$, $^{28,29}Si_2F_6$, and $^{28,28}Si_2F_6$ are proportional to the n-th power of the fluence, where n is 0.77 ± 0.07, 1.7 ± 0.2, and 2.1 ± 0.2, respectively. The n value increases with the frequency difference between the ν_7 or ν_{10} frequencies and the excitation laser frequency as a result of the decrease in the excitation rate to the quasi-continuum states. Figure 11 shows the dependence of the dissociation rates and enrichment factors on the fluence of the dissociation laser. The dissociation and excitation laser frequencies are also 954.55 and

	$^{28,30}Si_2F_6$	$^{28,29}Si_2F_6$	$^{28,28}Si_2F_6$
$\bar{n}_{ph}$	4.4	1.2	0.1
State Density at $\bar{n}_{ph}h\nu_{ex}$ ($/cm^{-1}$)	1.4×10^4	3	0.02

TABLE 2 Number of average absorbed photon ($\bar{n}_{ph}$) and state density at average excitation level ($\bar{n}_{ph}h\nu_{ex}$) of Si_2F_6 irradiated at the laser fluence of 0.068 J/cm^2 and the laser frequency of 966.23 cm^{-1}

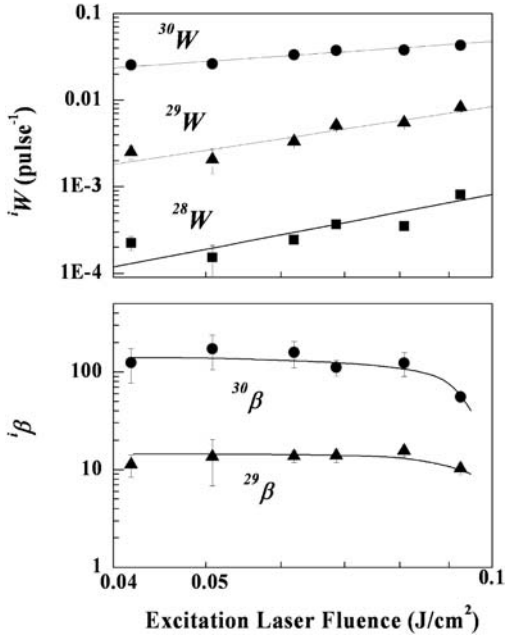

FIGURE 10 Dependence of dissociation rate ${}^{i}W$ and enrichment factor ${}^{i}\beta$ on excitation laser fluence. The excitation and dissociation laser frequencies are 966.23 and 954.55 cm^{-1}, respectively. The dissociation laser fluence is fixed at 0.90 ± 0.02 J/cm^2

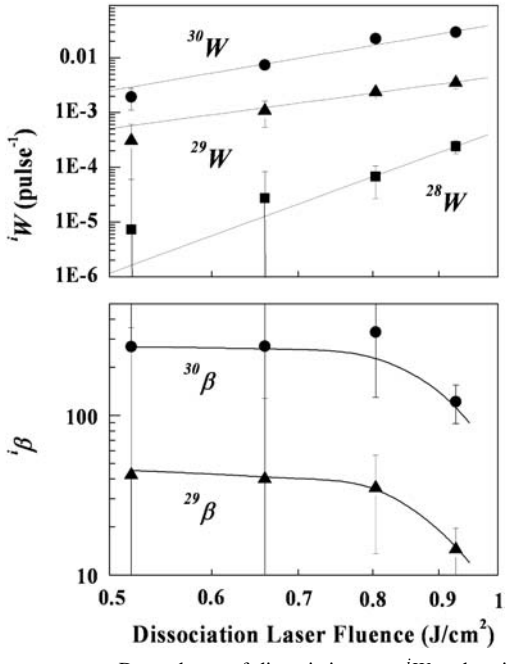

FIGURE 11 Dependence of dissociation rate ${}^{i}W$ and enrichment factor ${}^{i}\beta$ on dissociation laser fluence. The excitation and dissociation laser frequencies are 966.23 and 954.55 cm^{-1}, respectively. The excitation laser fluence is fixed at 0.063 ± 0.003 J/cm^2

966.23 cm^{-1} in this case, respectively. The excitation laser fluence is fixed at 0.063 ± 0.003 J/cm^2. The errors associated with the dissociation rate of $^{28,28}Si_2F_6$ are large at low dissociation laser fluences because of the small dissociation fraction. The dissociation rates show stronger dependence on the dissociation laser fluence than the excitation laser fluence; that is, n is 4.0 ± 0.4, 3.1 ± 1.7, and 8.7 ± 6.3 respectively for $^{28,30}Si_2F_6$, $^{28,29}Si_2F_6$, and $^{28,28}Si_2F_6$. Although the enrichment factors are nearly constant within the experimental errors at fluence below 0.8 J/cm^2, the factors decrease at higher fluence.

3.6 *Effect of two frequency irradiation scheme on separation efficiency*

As described in Sect. 3.1, ^{28}Si is enriched in Si_2F_6 by selectively dissociating Si_2F_6 containing ^{29}Si and ^{30}Si: $^{28,29}Si_2F_6$, $^{28,30}Si_2F_6$, $^{29,29}Si_2F_6$, $^{29,30}Si_2F_6$, and $^{30,30}Si_2F_6$. Therefore, it is essentially important for large scale production of highly enriched ^{28}Si to reduce the number of laser shots required to dissociate selectively all isotopic Si_2F_6 molecules except $^{28,28}Si_2F_6$ at such a low laser fluence that focus of the laser beam is not needed. Moreover, the yield of Si_2F_6, which is defined as the fraction of the amount of the remaining Si_2F_6 at the end of the enrichment process to the initial amount of Si_2F_6, is desirable to be as high as possible. Figure 12 shows the dependence of the ^{28}Si fraction in Si_2F_6 on the number of laser shots. In the case of two-frequency irradiation, Si_2F_6 was irradiated simultaneously with 966.23 cm^{-1} photons (0.089 J/cm^2) and 954.55 cm^{-1} photons (0.92 J/cm^2). On the other hand, Si_2F_6 was irradiated only with the 954.55 cm^{-1} photons at 0.92 J/cm^2. It is obvious that the two-frequency irradiation reduces remarkably the required number of shots even though the total laser fluence is almost same as that used in the single-frequency irradiation; that is, ^{28}Si fraction of 99.4% is obtained after 40.0% dissociation of Si_2F_6 by only 100 shots of two-frequency irradiation at total fluence of 1.01 J/cm^2, whereas 27.2% dissociation of Si_2F_6 by 1000 shots of single-frequency irradiation at 0.92 J/cm^2 is needed to make a ^{28}Si fraction in Si_2F_6 to be 99.0%. The corresponding yields of Si_2F_6 are 0.60 and 0.73 for two- and single-frequency irradiations, respectively. No detectable dissociation of Si_2F_6 was observed when Si_2F_6 was irradiated only with 966.23 cm^{-1} photons at 0.089 J/cm^2. Therefore, Si_2F_6 is only excited to quasi-continuum states below the dissociation level by the irradiation with 966.23 cm^{-1} photons at 0.089 J/cm^2. Although larger dissociation rate for ^{29}Si and ^{30}Si is obtained at the dissociation laser frequency of 956.19 cm^{-1} than at 954.55 cm^{-1} as shown in Fig. 7, laser fluence larger than 0.74 J/cm^2 could

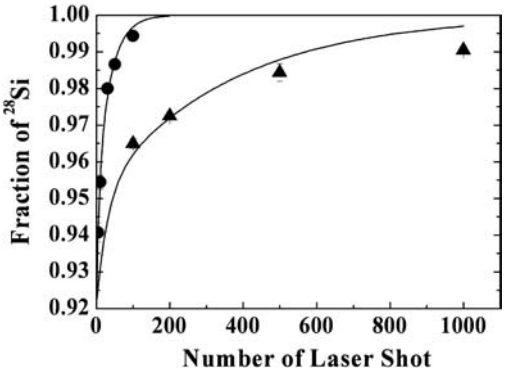

FIGURE 12 Laser shot dependence of ^{28}Si fraction in Si_2F_6 under single- (▲) and two-frequency (●) irradiation conditions. The Si_2F_6 pressure is 2 Torr both in single- and two-frequency irradiation. The excitation and dissociation laser frequencies are 966.23 and 954.55 cm^{-1}, respectively

not be obtained at 956.19 cm^{-1}, because the line ($10P(4)$-line) is at high frequency edge of the P-branch of the 10.6 μm band. Consequently, larger dissociation rates for ^{29}Si and ^{30}Si were obtained by the irradiation with 954.55 cm^{-1} photons at 0.92 J/cm^2 than by the irradiation with 956.19 cm^{-1} at 0.74 J/cm^2.

4 Conclusion

Laser silicon isotope separation has been done utilizing the isotopically selective IRMPD of Si_2F_6 under the two-frequency irradiation condition. The dissociation efficiency is enhanced significantly by the selective excitation of Si_2F_6 containing ^{29}Si and ^{30}Si to quasi-continuum states through ν_{10} vibrational mode at low laser fluence, followed by the dissociation of the molecules in the quasi-continuum states with the irradiation of the lower frequency laser photons at higher fluence. This enhancement would promise a practical large-scale separation, because focus of the laser beams is not needed. The Si_2F_6 pressure dependence of the dissociation rates shows that the enrichment factors for ^{29}Si and ^{30}Si increase with increasing pressure. It is plausible that this enhancement of the enrichment factors is due to the different behavior for the vibrational de-excitation from the quasi-continuum states during the laser pulse between the isotopic molecules.

REFERENCES

1 A. Yokoyama, H. Ohba, T. Shibata, S. Kawanishi, S. Sugimoto, T. Ishii, A. Ohya, Y. Miyamoto, S. Isomura, S. Arai: J. Nucl. Sci. Technol. **39**, 457 (2002)
2 P.L. Komarov, M.G. Burzo, G. Kaytaz, P.E. Raad: Microelectron. J. **34**, 1115 (2003)
3 T. Ruf, R.W. Henn, M. Asen-Palmer, E. Gmelin, M. Cardona, H.-J. Pohl, G.G. Devyatych, P.G. Sennikov: Solid State Comm. **115**, 243 (2000)
4 J.L. Lyman, S.D. Rockwood: J. Appl. Phys. **47**, 595 (1976)
5 M. Kamioka, S. Arai, Y. Ishikawa, S. Isomura, N. Takamiya: Chem. Phys. Letters **119**, 357 (1985)
6 M. Kamioka, Y. Ishikawa, H. Kaetsu, S. Isomura, S. Arai: J. Phys. Chem. **90**, 5727 (1986)
7 S. Arai, H. Kaetsu, S. Isomura: Appl. Phys. B **53**, 199 (1991)
8 K. Tanaka, S. Isomura, H. Kaetsu, Y. Yatsurugi, M. Hashimoto, K. Togashi, S. Arai: Bull. Chem. Soc. Jpn. **69**, 493 (1996)
9 Y. Okada K. Takeuchi: J. Nucl. Sci. Technol. **34**, 413 (1997)
10 J.L. Lyman, B.E. Newman, T. Noda, H. Suzuki: J. Phys. Chem. A **103**, 4227 (1999)
11 V.S. Letokhov: *Nonlinear Laser Chemistry* (Springer, Berlin 1983)
12 A.V. Evseev, V.S. Letokhov, A.A. Puretzky: Appl. Phys. B **36**, 93 (1985)
13 A. Yokoyama, K. Suzuki, G. Fujisawa, N. Ishikawa M. Iwasaki: Appl. Phys. B **38**, 99 (1985)
14 M.J. Frisch, et al.: GAUSSIAN 98 *(Revision A.3)*, (Gaussian, Inc., Pittsburgh PA, 1998)
15 V. Tosa, K. Ashimine, K. Takeuchi: J. Mol. Struct. **410–411**, 411 (1997)
16 S.K. Bains, P.N. Noble, R. Walsh: J. Chem. Soc. Faraday Trans. II **82**, 837 (1986)
17 R.V. Ambartzumian: Two-Frequency Technique for Multiple-Photon Dissociation and Laser Isotope Separation, In: *Multiple-Photon Excitation and Dissociation of Polyatomic Molecules*, ed. by C.D. Cantrell (Springer, Berlin 1986)
18 E. Alonso, J.A. O'Neill, L. Pateopol, B. Pogue: J. Phys. B **27**, 913 (1994)
19 P.A. Hackett, M. Gauthier, C. Willis, R. Pilon: J. Chem. Phys. **71**, 546 (1979)
20 M. Gauthier, W.S. Nip, P.A. Hackett, C. Willis: Chem. Phys. Letters **69**, 372 (1980)
21 V.S. Doljikov, Y.R. Kolomisky, E.A. Ryabov: Chem. Phys. Letters **80**, 433 (1981)
22 M. Gauthier, C.G. Cureton, P.A. Hackett, C. Willis: Appl. Phys. B **28**, 43 (1982)
23 K.A. Holbrook, M.J. Pilling, S.H. Robertson: *Unimolecular Reactions* 2nd edn. (Wiley, Chichester 1966)